Orientation of Liquid Crystalline Epoxides under ac Electric Fields

Atsushi Shiota† and Christopher K. Ober*

Department of Materials Science and Engineering, Bard Hall, Cornell University, Ithaca, New York 14853-1501

Received November 30, 1996; Revised Manuscript Received March 18, 1997[⊗]

ABSTRACT: The curing of liquid crystalline (LC) epoxides containing phenyl benzoate mesogens was studied under applied ac electric fields. When curing reactions began under a low-frequency electric field (∼1 V/μm), parallel molecular orientation slowly changed to perpendicular to the field, because a crossover (cutoff) frequency of molecular orientation shifted to much lower frequencies as the curing reaction took place. As a result, the cured networks possessed orientation perpendicular to the applied ac electric fields regardless of the initial frequency. Due to electrohydrodynamic effects, curing reactions under a low-frequency electric field proceeded faster than those at high frequency. Electric fields also affected formation of the LC structure, in particular, in smectic networks. Curing of LC epoxides with twin mesogen architecture under an ac electric field produced a smectic-A like structure with a fan shape-like texture, whereas curing without an external field formed a disclination rich texture. The oriented smectic network possessed high orientation as well as high translational order. The mechanical properties of the oriented smectic-like network showed a negative CTE as well as linear load-extension behavior in the rubbery regime. These characteristics can be explained in terms of the smectic layer spacing and the lateral spacing between mesogenic groups as confirmed by X-ray diffraction measurements.

Introduction

Formation of thermosets from liquid crystalline (LC) monomers is being used as a means of preparing materials with novel mechanical and optical properties.[1,2] As a result of their optical anisotropy, liquid crystals have potential in a wide range of applications including optical filters, displays, and data storage. Locking-in orientation by means of the formation of covalently bonded networks has enabled the creation of these new controlled-order materials. LC thermosets also offer the possibility of producing bulk layered structures with macroscopic orientation if cured in an aligning field. The study of such materials may provide insight into the behavior and creation of large dimension analogs to Langmuir−Blodgett films provided that smectic-like order can be formed in the network.

There exist several ways to obtain oriented networks from LC monomers. Broer[3] used surface alignment by rubbed polyimides, which are conventionally used for the LC display fabrication process. Barclay[4] and Jahromi[5] employed magnetic fields to align LC networks. Recently, Körner et al. also demonstrated that ac electric fields could be used in the processing of thin film, LC thermosets using a phenyl benzoate-type mesogen to produce cured network structures selectively oriented either parallel or perpendicular to a film substrate.[6] ac electric fields have advantages over dc electric fields in aligning networks because less ion migration can take place. This means that relatively strong electric fields may be applied, which are particularly effective for alignment when LC molecules with small dipole moments are used.

It is known that the domain formation and reorientation behavior of LC molecules under ac electric fields can be broadly described by electrohydrodynamic theory.[7] Of interest are how curing reactions of LC thermosets influence electrohydrodynamic effects and how alternating electric fields influence formation of network structure. It is thought that changes in electrohydrodynamic behavior during polymerization are mainly due to differences in the relaxation time of low molecular mass and polymeric systems. An increase of viscosity as polymerization proceeds causes important changes in relaxation of charge accumulation, which is associated with Carr−Helfrich processes.[8] Likewise, both the increase in viscosity and the change in molecular geometry cause significant changes in the Debye-type dielectric relaxation of the molecules. It is thought that the direction of molecular orientation either parallel or perpendicular to applied electric fields is dominated by the location of these two shifting critical frequencies. To clarify these issues, we prepared nematic diepoxy compounds composed of a phenyl benzoate mesogen, which itself has a larger transverse dipole component (2.4 Debye) than its longitudinal dipole component (1.2 Debye).

However, dielectric anisotropy is governed not only by a permanent dipole but also by molecular polarization, as explained by Meyer.[9] Because of this molecular polarization, the dielectric anisotropy of phenyl benzoate derivatives can range from negative to slightly positive. We therefore expect that changes in dielectric anisotropy may occur during polymerization as a result of the changing chemical structure.

We reported previously that 4-(4-oxiranylbutoxy)-benzoic acid 1,4-phenylene ester (CAS registry no. (supplied by authors): 153881-44-8), which we call **6e**, formed a nematic-like network when reacted with a diamine compound. On the other hand, 4-(oxiranylmethoxy)-benzoic acid 1,8-octanediylbis(oxy-4,1-phenylene) ester (CAS registry no. (supplied by authors): 173844-51-4), which we call **twin8e**, and 4-(oxiranylmethoxy)benzoic acid 1,9-nonanediylbis(oxy-4,1-phenylene) ester (CAS registry no. (supplied by authors): 173844-52-5), which we call **twin9e**, produced a smectic-like network when reacted with a diamine compound.[10] Using these monomers, formation of both nematic and

* To whom all correspondence should be addressed.
† Current address: Japan Synthetic Rubber Co., Ltd., Tsukuba Research Laboratory, 25 Miyukigaoka, Tsukuba-Shi, Ibaraki 305, Japan.
⊗ Abstract published in *Advance ACS Abstracts,* July 1, 1997.

S0024-9297(96)01745-7 CCC: $14.00 © 1997 American Chemical Society

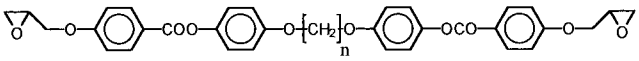

n = 8 : **Twin8e**
4-(Oxiranylmethoxy)benzoic acid 1,8-octanediylbis(oxy-4,1-phenylene) ester
CAS registry number : 173844-51-4
K 152 °C N 182 °C I

n = 9 : **Twin9e**
4-(Oxiranylmethoxy)benzoic acid 1,9-nonanediylbis(oxy-4,1-phenylene) ester
CAS registry number : 173844-52-5
K 127 °C N 149 °C I

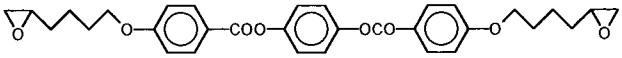

6e
4-(4-oxiranylbutoxy)benzoic acid 1,4-phenylene ester
CAS registry number : 153881-44-8
K 124 °C N 210 °C I

Figure 1. Structure of LC diepoxy monomers examined in this study.

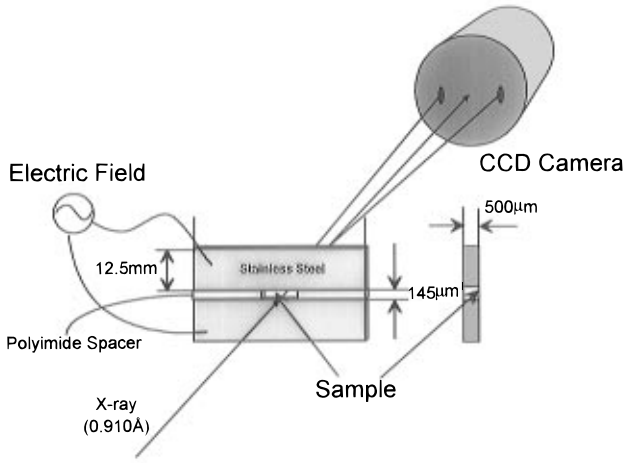

Figure 2. Scheme for real time X-ray diffraction experiments using ac electric fields.

smectic networks under ac electric fields was examined in detail and is described in the present paper. We also report development of unusual mechanical properties in these highly oriented smectic networks.

Experimental Section

The synthesis and purification of the LC diepoxy compounds for this study have been described previously.[10] Sulfanilamide (SAA) and diaminodiphenylmethane (DDM) purchased from Aldrich Chemical Co. were used as curing agents. SAA was used without further purification. DDM was used after recrystallization from ethanol. Stoichiometric amounts of the diepoxy monomer (2 mol) and the curing agent (1 mol) were ground in a mortar and pestle to produce the reactant mixture.

The real time X-ray diffraction data were obtained at the F1 beamline of the Cornell High Energy Synchrotron Source (CHESS). Sample cells consisted of two 500 μm wide stainless steel electrodes that were separated by a controlled gap spacing of 72.5 or 145 μm using a polyimide film (Figure 2). The cell was mounted in a Mettler FP-82HT hotstage to regulate the sample temperature. Voltage and frequency generated by an HP 8116A function generator were amplified 1000× by a Trek model 10/10 high-voltage operational amplifier and were applied to the cell. The flux of a monochromated beam of 0.910 Å wavelength provided 27 000 cps after being collimated by a 0.3 mm diameter collimator and allowed exposure times of less than 1 s. X-ray diffraction images were recorded on a flat CCD detector every 30−40 s, including data transfer and processing time, and were finally saved as 16 bit resolution images in tiff format.

Orientation parameters were calculated from azimuthal scans passing through the wide angle reflections on the flat

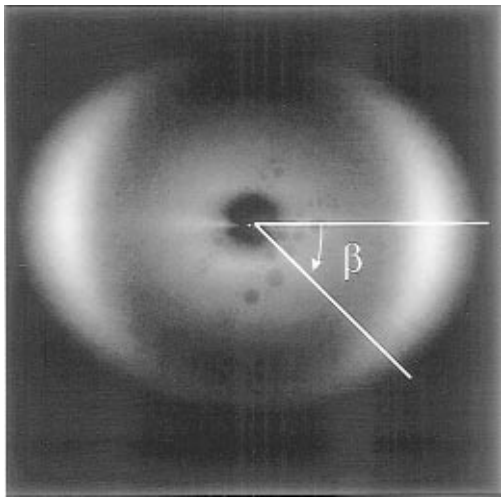

Figure 3. Calculation of the orientation parameter for the azimuthal scan of an X-ray diffraction image.

images, by the Hermans' method.[11,12] The distribution in intensity (I) as a function of angle (β) for a given quadrant of the azimuthal scan was obtained. Intensity maxima were set at an angle of $\beta = 0°$. (Figure 3). Conversion of the $I(\beta)$ data to $I(\alpha)$ was accomplished using the relationship from spherical trigonometry shown in

$$\cos(\alpha) = \cos(\beta)\cos(\theta_B) \tag{1}$$

where θ_B is the Bragg angle and α is the angle between the normals to the scattering planes and the electric field direction. To calculate the average cosine square of α, integration of the $I(\alpha)$ data versus α was performed using

$$\langle\cos^2\alpha\rangle = \frac{\int_0^{\pi/2} I(\alpha)\sin(\alpha)\cos^2(\alpha)\,d\alpha}{\int_0^{\pi/2} I(\alpha)\sin(\alpha)\,d\alpha} \tag{2}$$

From sample geometry, we know that the summation of the average angles between the x, y, and z axes and the director must equal 1. If we assume cylindrical symmetry of the long axis of the molecules, one can relate $\langle\cos^2\alpha\rangle$ to the average angle of interest, $\langle\cos^2\varphi\rangle$, the average angle between the axis of the structural unit and the director, using

$$\langle\cos^2\varphi\rangle = 1 - 2\langle\cos^2\alpha\rangle \tag{3}$$

The director orientation parameter, S, is calculated using

$$S = \frac{3\langle\cos^2\varphi\rangle - 1}{2} \tag{4}$$

Orientation parameters reported are the average of the four orientation parameters calculated for each image quadrant.

Equations 1−4 were also applied to evaluate the orientation of the smectic layer diffraction. The Herman equations are not by definition intended to calculate orientational order in a smectic layer diffraction. However, it is convenient to obtain numerical information concerning orientation from the smectic layer. The orientation parameter for the smectic layer is denoted by S_s in the present paper.

A TA Instruments 910 differential scanning calorimeter (DSC) was used in order to obtain the extent of polymerization, which was calculated as a ratio of the partial heat of reaction and overall heat of reaction.[13]

In order to measure mechanical properties of the cured LC diepoxide, film-shaped specimens with 500 μm (W) × 150 μm (T) × 12.5 mm (L) were prepared in a stainless mold. And then the specimens were subjected to a thermomechanical analysis (TMA), stress−strain measurement, and dynamic mechanical analysis (DMA).

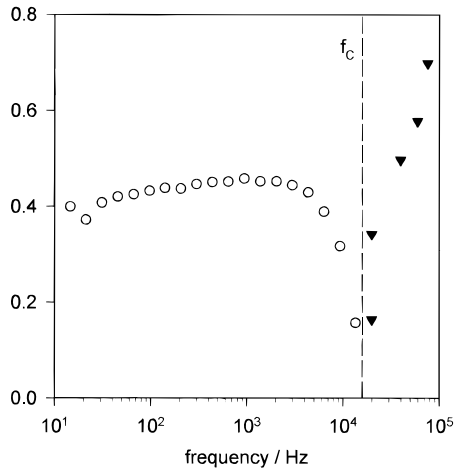

Figure 4. Frequency dependence of the orientation parameter (S) for the **6e** molecule at 140 °C. A 1 V/μm electric field was applied. (○) The director was set along the electric field. (▼) The director was set perpendicular to the electric field.

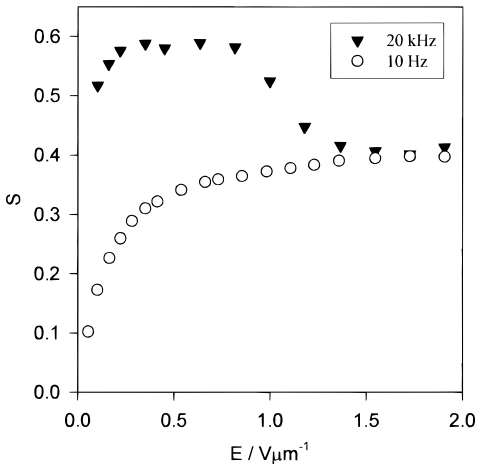

Figure 5. Dependence of the orientation parameter (S) of **6e** upon the strength of the electric field at 120 °C. (○) An electric field of 10 Hz was applied; the director was set along the electric field. (▼) An electric field of 20 kHz was applied; the director was set perpendicular to the electric field.

A TA Instruments 943 thermomechanical analyzer was employed for measurement of thermal expansion of the networks. The measurement was carried out in a film extension mode with a 5 mN static tension and a heating rate of 4 °C/min. A Perkin-Elmer DMA-7 was used for both stress−strain measurement and dynamic mechanical measurement. Stress−strain measurements were carried out with an increasing stress of 250 mN/min up to 2.5 N. Dynamic mechanical measurements were carried out with a frequency of 10 Hz, a strain of 0.1%, and a heating rate of 4 °C/min.

Results and Discussion

Nematic Networks. We previously reported that curing of LC epoxy monomer **6e** with a diamine compound resulted in a nematic-like network.[10] The epoxy **6e** provides a moderate curing rate over a 120−180 °C temperature range because of its low reactivity, allowing for various real-time measurements to be carried out. First of all, let us briefly describe the orientation behavior of molecule **6e** under ac electric fields. Figure 4 shows dependence of the orientation parameter (S) upon the frequency of an applied electric field for the **6e** molecule at 140 °C. The figure shows that **6e** aligns parallel to the electric field below 10 kHz, while the molecule aligns normal to the electric field above 20 kHz. Switching of the orientation can be ascribed to an electrohydrodynamic effect. The electrohydrodynamic equation,[7] which is composed of the anisotropic conductivity ($\sigma_a = \sigma_{||} - \sigma_\perp > 0$), anisotropy of the dielectric constant ($\epsilon_a = \epsilon_{||} - \epsilon_\perp$), anisotropic magnetic susceptibility ($\chi_a = \chi_{||} - \chi_\perp$), the twist viscosity ($\gamma_1$),[14] and the Miesowicz viscosity coefficients ($\eta_0 = (\eta_1 + \eta_2 - \gamma_1)/2$),[15] describes the relationship between a crossover frequency f_C ($=\omega_C/2\pi$), a stability−instability threshold of the applied electric field (E_{th}), and the above anisotropic parameters.

$$E_{th}^2(\omega) = E_0^2 \frac{1 + \omega^2\tau^2}{\zeta^2 - 1 - \omega^2\tau^2} \tag{5}$$

$$E_0^2 = -\frac{4\pi\epsilon_{||}}{\epsilon_a\epsilon_\perp}(\chi_a H^2 + K_{33}k^2) \tag{6}$$

K_{33} is the elastic coefficient of bend, $k = \pi/d$, where d is the sample thickness.

$$\omega_C = (\zeta^2 - 1)^{1/2}/\tau \tag{7}$$

ζ^2 is the Helfrich parameter, characteristic of the material, defined by

$$\zeta^2 = \left(1 - \frac{\epsilon_{||}}{\epsilon_a}\frac{1}{1 + \eta_0/\gamma_1}\right)\left(1 - \frac{\sigma_\perp\epsilon_{||}}{\sigma_{||}\epsilon_\perp}\right) \tag{8}$$

τ is the relaxation time for the space charge:

$$\tau^{-1} = 4\pi\sigma_{||}/\epsilon_{||} \tag{9}$$

The region below f_C is called the "conduction regime"[7] because convection of the charge density dominates the instabilities, domain formation, and reorientation. The region above f_C is called the "dielectric regime", where the charge density becomes time-independent. The charges accumulated by the Carr−Helfrich process do not have enough time to follow the cycle of the applied alternating field. It is thought that in the dielectric regime, a transverse component of the dipole couples directly to the applied electric field, while in the conduction regime, convective flow and charge accumulation drive molecules to homeotropic orientation. Dependence of molecular orientation upon the strength of ac electric fields in the dielectric regime is in contrast to that under the conduction regime. An orientation parameter (S) can be described by an exponential function of strength of electric fields (E) in the conduction regime. On the contrary, in the dielectric regime, S decreased above E_{th} to approximately 1 V/μm due to an instability (see Figure 5). The details of the electrohydrodynamic affects for phenyl benzoate derivatives were also recently reported.[16]

Of interest was how the curing reactions of the LC epoxy were affected by the electrohydrodynamic effect. Figure 6 shows changes in orientation parameter during an isothermal curing reaction of **6e**/DMM at 140 °C under an electric field of 10 Hz and 1 V/μm. At the beginning of the curing reaction, the molecules were aligned along the electric field. However, orientation became worse as the reaction proceeded; eventually, molecular orientation became perpendicular to the electric field approximately 15 min after starting the curing reaction. Figure 7 illustrates that f_C shifted downward exponentially as the reaction proceeded. The extent of polymerization calculated from the corresponding isothermal DSC experiment indicates that f_C

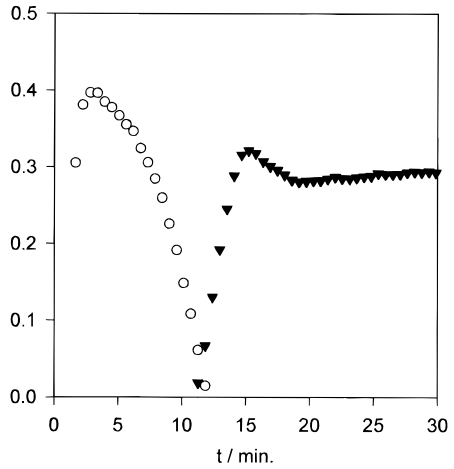

Figure 6. Changes in orientation parameter (S) during the isothermal curing reaction of **6e**/DDM at 140 °C under an electric field of 10 Hz and 1 V/μm. (○) The director was set along the electric field. (▼) The director was set perpendicular to the electric field.

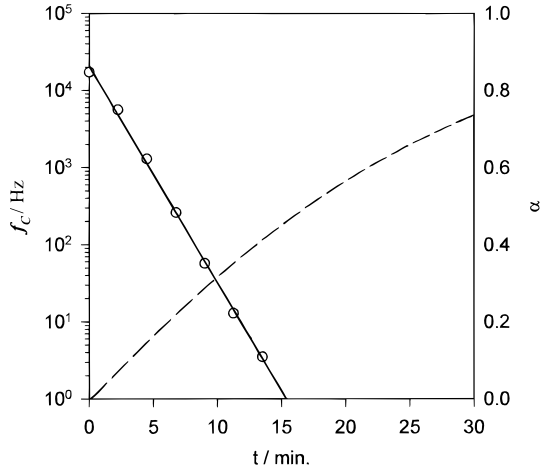

Figure 7. Changes in crossover frequency (f_C, solid line) and extent of polymerization (α, broken line) during the isothermal curing reaction at 140 °C as a function of curing time.

reaches 1 Hz at a conversion of approximately 0.45 and a curing temperature of 140 °C. For the reaction of a diepoxy and an amine, gelation is expected to occur at a conversion of approximately 0.58. This means whenever the curing reaction starts in the conduction regime, a 90° orientation flip takes place before gelation. The shift of f_C can be attributed to an increase of viscosity as explained in eqs 7 and 8. Likewise, molecular size may affect polarization, which is an important component of the dielectric anisotropy of the system.

These results are in contrast to those on the curing of nematic dicyanate ester monomers under ac electric fields, in which it is possible to select orientation either parallel or perpendicular to the applied electric field.[6] It is thought that, in the LC dicyanate ester system, shifting of f_C is smaller during curing and, in addition, gelation occurred more abruptly than in the LC epoxy system. These differences may be ascribed to the topology of network formation. It is thought that the polymerization proceeds linearly before gelation in the LC epoxy system while network formation in the LC dicyanate system involves a more highly branched structure due to triazine ring generation. A high aspect ratio, high molecular weight molecule possesses a longer response time to an external field than a spherical molecule of modest molecular weight. Likewise, Chien et al. suggested that the existence of a spacer may help to develop physical interaction between chains.[17] Therefore, a modest molecular weight LC epoxy structure behaves as though it were larger and increases viscosity faster than the LC dicyanates system. As a result of these effects, we believe that, in the LC epoxy system, f_C drops to less than 1 Hz before gelation.

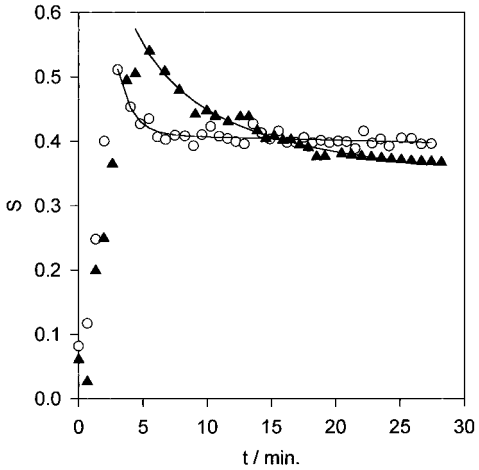

Figure 8. Changes in orientation parameter (S) during the isothermal curing reaction of **6e**/DDM at 140 °C (○) and **6e**/SAA at 175 °C (▲) under an electric field of 20 kHz and 0.75 V/μm.

When the curing reaction was carried out in the dielectric regime, the initial orientation could be fixed in the network. However, polymerization caused a decrease of orientation. Under an electric field of 20 kHz and 0.75 V/μm at 140 °C, the reactant mixture initially showed an orientation parameter close to 0.55. The orientation decreased as the reaction continued, eventually saturating at 0.4 (see Figure 8). A similar result was obtained for curing of **6e** with SAA at 175 °C. It is understandable for a liquid crystalline thermoset that network formation causes a more defective structure. The stimulated thermal motion of reactive sites favors the construction of disordered networks, while anisotropic dispersion interactions and steric packing interactions act to retain the mesophase.

A curing reaction performed in the dielectric regime tended to yield better orientation than when curing started in the conduction regime. An orientation parameter of 0.40 was obtained when **6e**/DDM was cured at 140 °C under an electric field of 20 kHz and 0.75 V/μm, while an orientation parameter of 0.29 was obtained at the same temperature and strength of electric field but at 10 Hz. Molecular motion in the dielectric regime is relatively static because the dipole moment of the molecule is coupled to an applied electric field, whereas molecular motion is strongly activated and even dynamic flow takes place in the conduction regime.

Smectic Networks. It was possible to monitor evolution of the smectic structure during the curing of a twin epoxy monomer and a diamine in real time. A combination of **twin8e** (T_N 152 °C) and SAA (T_m 165 °C) provides a moderate reaction rate over a temperature of 160−200 °C. We reported that a combination of **twin8e**/SAA started to form a smectic phase at a conversion of approximately 0.25.[18] Then, the smectic structure was finally locked in a network. Figure 9A shows evolution of X-ray diffraction from the smectic layer during isothermal curing at 170 °C under an electric field of 10 Hz and 1 V/μm as well as 10 kHz

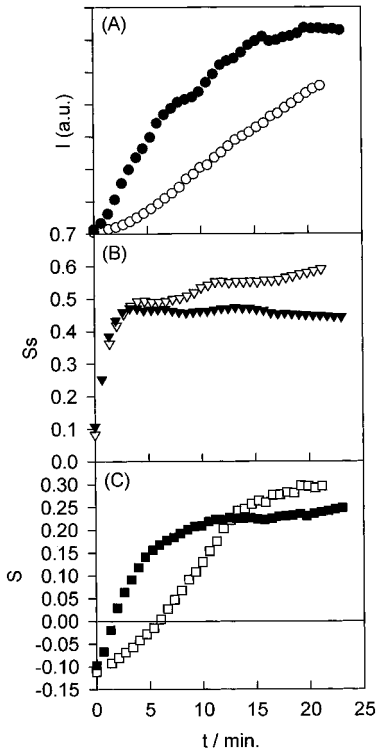

Figure 9. Isothermal curing reaction of **twin8e**/SAA at 170 °C under electric fields of 1 V/μm and 10 Hz (filled symbol) and 10 kHz (open symbol). (A) Changes in smectic layer diffraction intensity (d-spacing = 44 Å) upon horizontal scan (perpendicular to the electric field): (●) 10 Hz; (○) 10 kHz. (B) Changes in orientation parameter (S_s) for smectic layer diffraction: (▼) 10 Hz; (▽) 10 kHz. The director of the smectic layer was set parallel to the electric field. The figure shows that the smectic layers were aligned parallel to the electric field. (C) Changes in orientation parameter (S) for wide angle diffraction: (■) 10 Hz; (□) 10 kHz. The director was set perpendicular to the electric field. The figure shows that molecules are weakly aligned parallel to the electric fields initially and then aligned perpendicular to the electric fields.

and 0.75 V/μm. The figure illustrates that the increase of smectic layer diffraction intensity under a 10 kHz electric field occurred slower than under a 10 Hz electric field. In the **twin8e**/SAA system, the intensity change of smectic layer diffraction corresponds to the extent of curing. The **twin8e**−SAA adducts and network exhibit a smectic structure, whereas the **twin8e**/SAA mixture itself shows both nematic and isotropic phases initially. It therefore appears that the frequency of the electric field influenced the reaction rate. We believe that reaction rate was enhanced under a low-frequency electric field by electrohydrodynamic effects. As described in the nematic network section above, our investigations were performed under conditions of Debye type dielectric response; that is, molecules are able to follow the frequency of the alternating electric field. In the conduction regime, the **twin8e**/SAA system possesses a positive dielectric anisotropy in the initial stage of the reaction. This means that the low-frequency electric field can induce a molecular flipping motion. This molecular motion can even result in a local convective flow. We think that this activated molecular motion contributed to an increased frequency factor for the reaction and resulted in a faster reaction. For the same reason, we can see clear differences in the evolution of smectic layer diffraction between reactions conducted under an electric field at low frequency and curing performed without an electric field (see Figure 10).

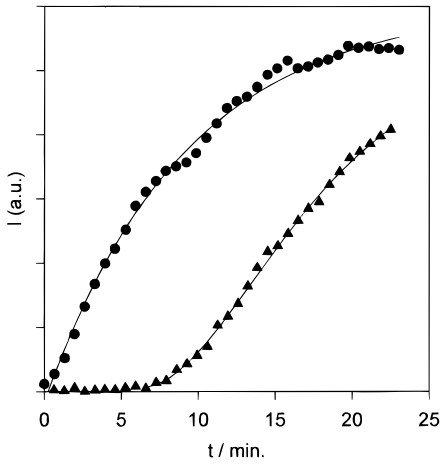

Figure 10. Changes in the intensity of the smectic layer diffraction of **twin8e**/SAA under isothermal curing at 170 °C: (●) under an electric field of 10 Hz and 1 V/μm; (▲) without an electric field.

The reactant mixture of **twin8e**/SAA displays a nematic phase below 175 °C and an isotropic phase above 175 °C.[18] This means when the curing reaction of **twin8e**/SAA was carried out below 175 °C, the thermoset system forms a nematic phase first and then goes into a smectic phase. Figure 9C shows changes in orientation for wide angle diffraction during the isothermal curing reaction at 170 °C under a 10 Hz electric field and a 10 kHz electric field. Because f_C of **twin8e** is close to 100 kHz at 170 °C, under both the 10 Hz and 10 kHz electric fields, the molecules are weakly aligned parallel to the electric field initially. Subsequently, the orientation of the molecules became perpendicular to the electric field.

However, while the wide angle diffraction oriented parallel to the applied electric field (Figure 9C), the smectic layer diffraction is also oriented parallel to the electric field (Figure 9B). These two facts contradict each other because reaction products of the **twin8e**/SAA possess a smectic-A phase. In a smectic-A phase, the orientation of the wide angle diffraction and smectic layer diffraction should be orthogonal. This contradiction can be resolved if we consider that the **twin8e**/SAA system is phase separated and that the smectic portion is aligned perpendicular to the electric field while the nematic portion is aligned parallel to the electric field. Actually, we reported that, as a result of POM (crossed polarizing optical microscope) investigations, the **twin8e**/SAA system exhibited a nematic−smectic biphase for a short time period in the intermediate stage of the reaction.[10] Likewise, de Jeu et al. reported for azoxybenzene derivatives that a phase transition from a nematic phase to a smectic phase simultaneously caused a sign change of dielectric anisotropy from negative to positive due to the change of molecular polarization.[19] It is thus possible that a smectic portion and a nematic portion can align in different directions simultaneously. As a result of these effects, orientation in the wide angle diffraction changed gradually from parallel to perpendicular with respect to the electric field as the smectic component increased because the wide angle diffraction has contributions from the nematic portion where the mesogens are aligned parallel to the electric field and the smectic portion where mesogens are aligned perpendicular to the electric field. On the contrary, the small angle smectic layer orientation showed a high value as soon as smectic diffraction emerged. When

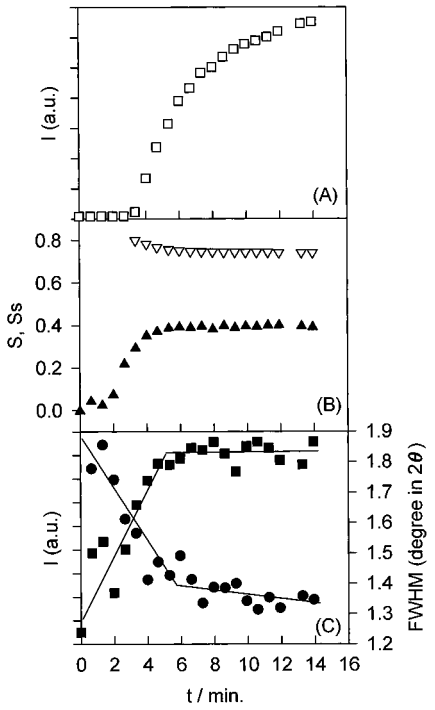

Figure 11. Isothermal curing reaction of **twin9e**/DDM at 140 °C under electric fields of 10 kHz and 0.75 V/mm. (A) Changes in smectic layer diffraction intensity upon horizontal scan (perpendicular to the electric field). (B) Changes in orientation parameters. (▽) S_s. The director of the smectic layer was set parallel to the electric field. The figure illustrates that the smectic layer was aligned parallel to the electric field. (▲) S. The director was set perpendicular to the electric field. The figure shows that molecules are aligned perpendicular to the electric field 3 min after the start of the reaction. (C) Changes in intensity (■) and full width at half-maximum (●) of the wide angle diffraction upon vertical scan (parallel to the electric field).

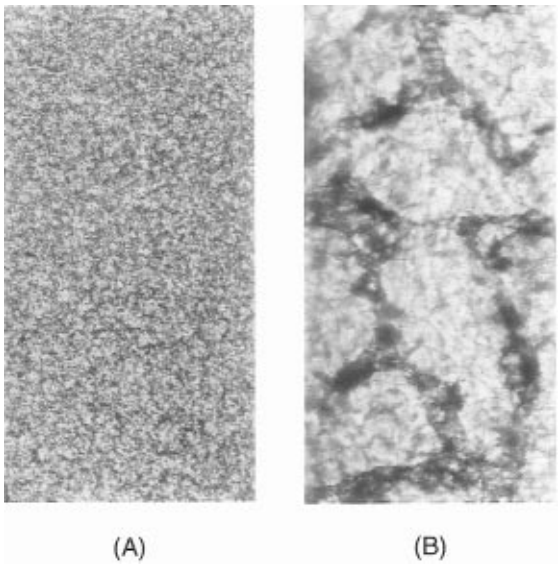

Figure 12. Optical texture of cured **twin9e**/DDM at 140 °C for 1 h: (A) cured without electric field; (B) cured under an electric field of 20 kHz and 0.75 V/μm.

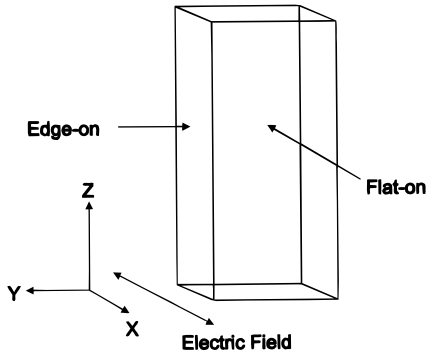

Figure 13. Geometry of the oriented film for X-ray diffraction experiments.

curing of **twin8e**/SAA is conducted above 175 °C, a smectic phase forms directly from an isotropic phase, as clearly observed by POM. In this case, no parallel orientation to the electric field was observed. Orientation in the wide angle diffraction increased gradually as the reaction proceeded because the wide angle diffraction consists of contribution from both the isotropic and smectic melts. Jahromi reported an increase of orientational order as the curing reaction proceeds in a 4-[2-(oxiranylmethoxy)ethoxy]benzoic acid 1,4-phenylene ester/4,4′-diaminobiphenyl system, which involves a nematic−smectic transition during the polymerization.[5] These results are in contrast to the results of the nematic system (**6e**/DDM) in which a decrease of orientation was observed as the reaction proceeds.

Evolution of the smectic structure was studied in detail in a mixture of **twin9e** and DDM because of its moderate reaction rate between 130 and 150 °C. Similar results to the **twin8e**/SAA system as described above were also obtained for the **twin9e**/DDM system (see Figure 11). According to POM observations, a smectic phase formed directly from an isotropic phase after a small extent of polymerization. The transition from the isotropic to the smectic state seemed to occur more suddenly in the **twin9e**/DDM system than in the **twin8e**/SAA mixture. As soon as the smectic phase appeared, orientation in the wide angle diffraction increased quickly and then remained constant. In the **twin9e**/DDM system, a phase transition was observed even in the wide angle diffraction as an increase of intensity and a decrease of full width at half-maximum with associated coherent length.

The **twin9e**/DDM formed an optical texture with dense disclination lines (see Figure 12A). Our interest included how the rich disclination structure was affected by an ac electric field when the **twin9e**/DDM mixture formed a network. For this purpose, oriented networks cured between two electrodes, as shown in Figure 2, were prepared. Subsequently, the oriented networks were removed from the electrodes; then, X-ray diffraction images were taken along three directions, as illustrated in Figure 13. Parts A (wide angle) and B (small angle) of Figure 14 show X-ray diffraction patterns for the **twin9e**/DDM cured at 145 °C under an electric field of 10 kHz and 0.75 V/μm, taken from the x-direction (edge-on side). As the figure shows under an ac electric field, the **twin9e**/DDM yielded a high orientation parameter of 0.409 ± 0.025 for a densely cross-linked network. The X-ray pattern taken from the z-direction also showed the same results. Figure 14C (wide angle) shows an X-ray diffraction image for the same sample, but the picture was taken from the y-direction (flat-on side). From the flat-on side, no orientation was observed. Orientation in the longitudinal direction could not be controlled because only transverse components of the dipole moment of the phenyl benzoate mesogens could couple to applied electric fields. In order to obtain three-dimensional orientation, an additional orientation technique such as

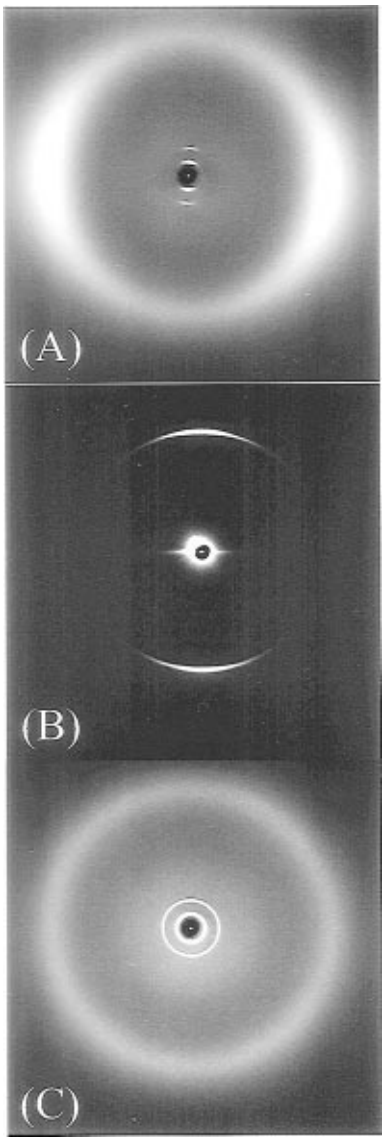

Figure 14. X-ray diffraction images of **twin9e**/DDM cured at 140 °C under an electric field of 20 kHz and 0.75 V/μm. (A) Wide angle diffraction image taken from the edge-on side. The molecules are well oriented perpendicular to the applied electric field. (B) Middle angle diffraction image take from the edge-on side. (C) Wide angle diffraction image taken from the flat-on side. The molecules are not oriented.

surface orientation using rubbed polyimide film may be required. Parts A and B of Figure 15 show azimuthal scans for the wide angle diffraction (2θ = 12.01°, d-spacing = 4.48 Å) and the smectic layer diffraction (2θ = 1.20°, d-spacing = 44.0 Å), respectively. These results clearly show that the network possesses a smectic-A like structure. Figure 12B shows an optical texture observed from the flat-on side of the oriented smectic network. A fan-shaped texture, which is consistent with a smectic-A phase, corresponds well with the X-ray diffraction results, whereas the optical texture for an unoriented network showed only dense disclination lines. These results indicate that an external electric field certainly affects the domain size and defect structure of the network.

Mechanical Properties of Oriented Smectic Networks. Mechanical properties of the oriented networks from **twin9e**/DDM shown in Figures 12(A)−15 are examined. Figure 16 displays stress−strain behavior of the oriented network as well as an unoriented network. For oriented samples, a strain was applied

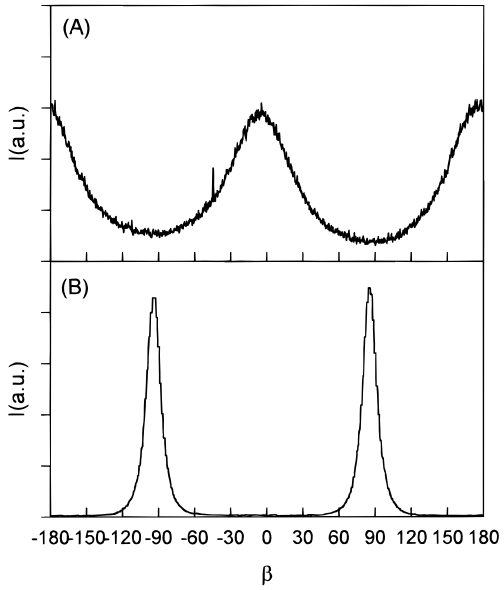

Figure 15. Distribution function (azimuthal scan) for diffractions scanned from Figure 14A: (A) wide angle diffraction at 2θ = 12.01°; (B) smectic layer diffraction at 2θ = 1.20°.

along the long direction of the specimen (parallel to the orientation). At room temperature, the oriented network showed similar stress−strain behavior with slight yielding to the unoriented network. However, at 80 °C ($< T_g$ = 118 °C), the oriented network displayed linear elasticity, while a yielding process could still be seen in the unoriented network. In the rubbery regime, the oriented network showed a higher modulus of 40 MPa at 2.5% strain than that of 32 MPa for the unoriented network, even though in the glassy regime, the oriented network had a lower modulus. Likewise, linear elasticity was seen in the oriented network. Jahromi et al.[20] reported a value of rubbery elastic modulus (E_r) for a similar system with comparison to theoretical predictions using the classical rubber elasticity theory.[21] The experimental value of E_r for an oriented LC network made from 4-[2-(oxiranylmethoxy)ethoxy]benzoic acid 1,4-phenylene ester/DDM showed a value 1.7 times higher than the theoretical value. In the same manner, E_r of 40 MPa for the oriented **twin9e**/DDM was also 1.7 times higher than the theoretical value of 24 MPa, while E_r for the unoriented **twin9e**/DDM only was 1.3 times higher.

In results from dynamic mechanical analysis (DMA) measurements, an obvious difference could be seen between the oriented and the unoriented network. A relatively strong sub-T_g transition, clearly separated from the α-relaxation, was observed between 50 and 100 °C only for the oriented network (see Figure 17).

Figure 18 displays the thermal expansion behavior for networks from **twin9e**/DDM in three different orientations. In the glassy regime, a highly oriented network (S = 0.455) possesses a low coefficient of thermal expansion (CTE) of 3.0×10^{-5} °C^{-1}. This value is as low as the CTE for a rigid-rod polymer such as an aromatic polyimide. In addition, Figure 18 shows that the highly oriented network possesses a negative CTE value in the rubbery regime. This suggests that, while the lateral distance expands, simultaneous shrinkage takes place along the director in the rubbery regime. This negative CTE is often observed in a highly oriented fiber or a film. Hikmet et al.[22] and Jahromi[20] also reported a negative CTE for a LC network in the direction parallel to the orientation. Consequently, a

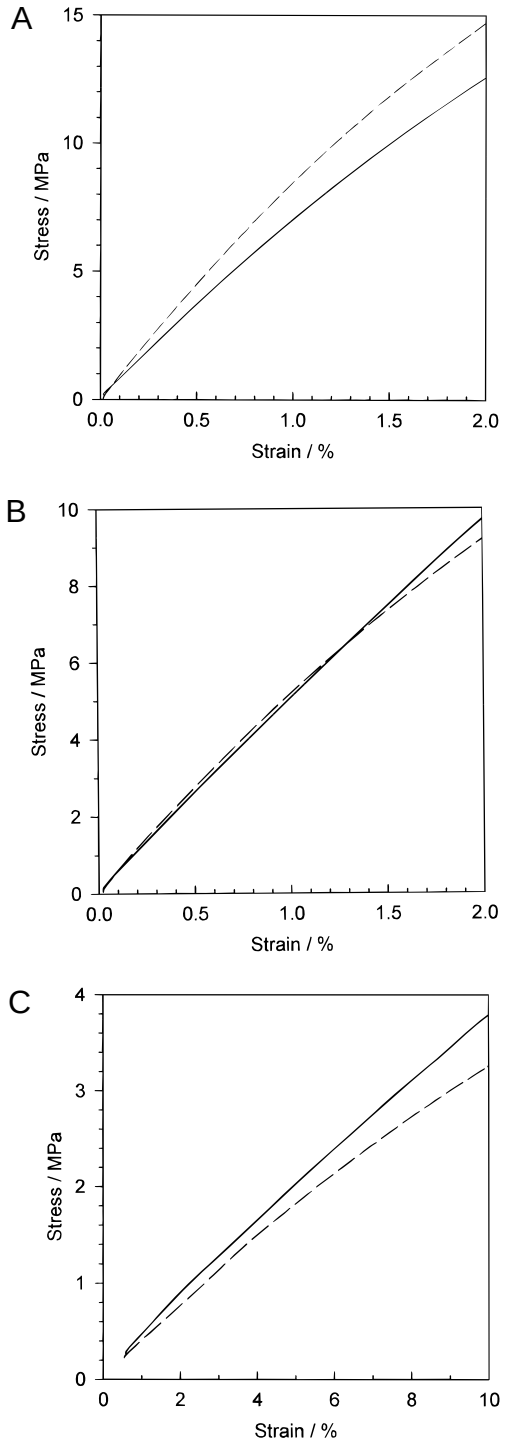

Figure 16. Load-extension behaviors of the oriented LC network with $S = 0.410$ (solid line) and the unoriented LC network (broken line) prepared from **twin9e**/DDM: (A) at 30 °C; (B) at 80 °C; (C) at 140 °C.

network with an orientation parameter of 0.29 displayed zero expansion in the rubbery regime because the shrinkage in the longitudinal direction and the expansion in the lateral direction were balanced. Dependence of the CTE in both the glassy and rubbery regimes upon S is linear (see Figure 19).

Also studied were changes in the X-ray diffraction pattern versus temperature (see Figure 20). Small changes in both wide angle and smectic layer diffraction as a function of temperature were successfully observed using a high-resolution CCD camera. We observed that the changes in *d*-spacing were thermally reversible and corresponded well with thermomechanical behavior. The

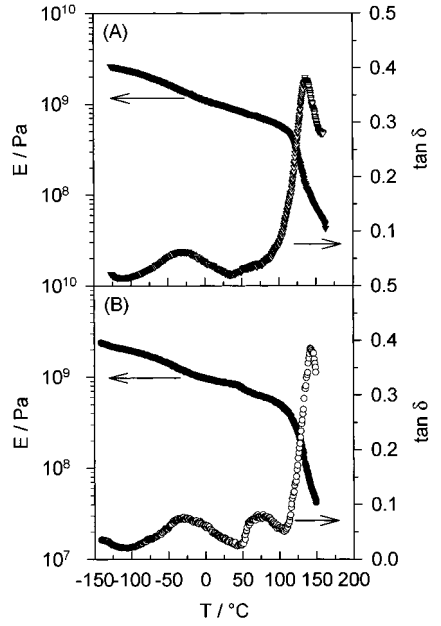

Figure 17. Dynamic mechanical measurements for (A) the unoriented network and for (B) the oriented LC network with $S = 0.430$ prepared from **twin9e**/DDM.

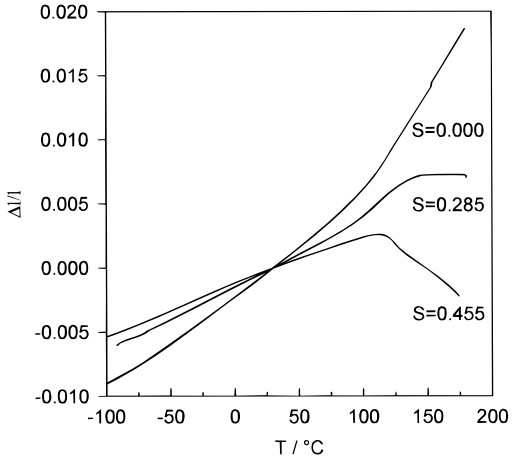

Figure 18. Thermal expansion behavior for the LC network from **twin9e**/DDM with various orientation parameters.

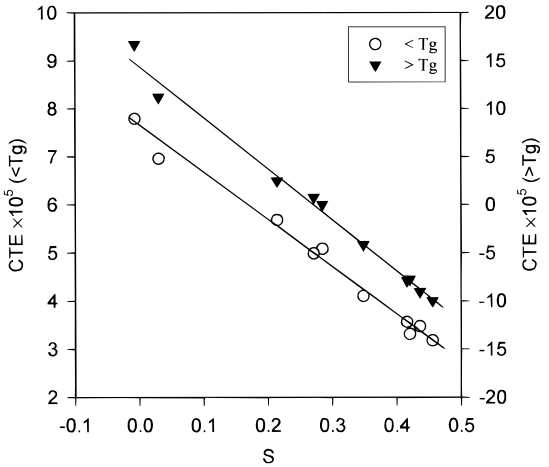

Figure 19. Relationship between the coefficient of thermal expansion (CTE) and the orientation parameter (S) for the LC network from **twin9e**/DDM.

oriented network possesses a narrower lateral distance and a wider smectic layer distance than the unoriented network. From 25 to 160 °C, the lateral distance for

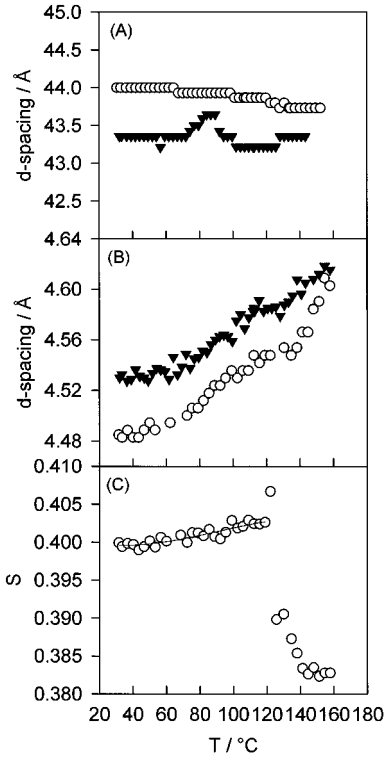

Figure 20. Temperature dependencies of the smectic layer spacing (A), lateral distance (B), and orientation parameter (S) (C) for the oriented network with $S = 0.400$ (open symbols) and the unoriented network (filled symbols) prepared from **twin9e**/DDM.

the oriented network expanded 0.12 Å (4.48 Å → 4.60 Å), whereas that for the unoriented network only expanded 0.80 Å (4.53 Å → 4.61 Å). This difference is mainly ascribed to a large expansion in the rubbery regime for the oriented network. While the lateral distance of the oriented network increased as the temperature rose, the smectic layer distance gradually and continuously decreased. However, the change of 0.25 Å in the 44 Å layer distance was extremely small compared to the changes in the lateral distance. On the other hand, changes in the smectic layer distance of the unoriented network displayed complicated behavior. The smectic layer distance increased suddenly at ~85 °C, then decreased up to the T_g, and subsequently, slightly increased again. For the oriented network, a sudden decrease of the orientation was observed above T_g.

It is thought that the above characteristics are strongly associated with each other. The temperature dependence of the mechanical properties of polymers can be understood as several relaxation processes that correspond to changes in molecular motion. Thus, anisotropy in the molecular packing may lead to differences in longitudinal and transverse components of the molecular relaxation as well as of the mechanical properties. Changes in thermomechanical behavior we noted were mainly associated with two relaxation process occurring at 50−100 °C (sub-α-process) and 110−130 °C (α-process). The sub-α-process was observed not only in the DMA measurement of the oriented network but also in the changes in *d*-spacing evaluated by X-ray diffraction measurements. For both oriented and unoriented networks, from ~50 to 100 °C, a large increase of the lateral spacing of approximately 0.5 Å was observed even below T_g. This increase of the lateral distance is distinct from another large increase above T_g, with a narrow plateau region located between ~100 and ~125 °C.

We believe that relaxation of strong intermolecular interactions between phenyl benzoate mesogens permits a change in the torsional angle between the phenyl benzoate mesogens and the spacer, resulting in the sub-α-relaxation. Because of a polydomain structure in the unoriented network, the sub-α-relaxation was reflected in changes in the smectic layer distance that showed a small peak between 70 and 100 °C. It is thought that changes in lateral distance influenced the smectic layer distance. The wider lateral distance of the unoriented network indicates that there exists less intermolecular interaction, which may explain the luck of clear sub-α-relaxation observed in the DMA measurement. Above the sub-α-relaxation, the oriented network shows linear stress−strain behavior. This suggests that the external stress was directly transmitted to the molecular axes. Thermal motion mainly distributed to the transverse direction of the molecular axis causes an increase of lateral distance and simultaneously causes a decrease of the smectic layer distance. This phenomenon even starts upon the sub-α-relaxation for the oriented network. Likewise, it is believed that the thermal fluctuation causes a decrease of the orientation above T_g.

Conclusion

The ability to create anisotropic network structures with selected orientation offers opportunities in the creation of new materials with tailored physical properties. Prior work on LC dicyanate thermosets has shown that it is possible to use electric field alignment to produce oriented networks. In the case of the LC epoxy thermosets, since the extent of polymerization has strongly influenced the molecular response to ac electric fields, the final networks could be aligned only perpendicular to the electric field in both the smectic and nematic networks. This is true even though the nematic epoxy monomers could be selectively oriented either parallel or perpendicular to the electric fields by simply switching the electric field frequency.

The oriented networks possessed some differences from unoriented networks in their relaxation behavior. An additional sub-T_g transition that could be observed by both DMA and X-ray measurements was attributed to relaxation of the interaction between mesogenic groups. Starting the curing reaction in the dielectric regime under 0.2−1 V/μm electric fields yielded the strongest orientation in the network because the initial orientation could be fixed. It is evident from the contrast in the behavior to other LC networks that it is necessary to take into account the topology of the growing network in order to predict the behavior of an "orientation-on-demand" thermoset system. However, it was demonstrated successfully through this study that a well-oriented smectic network can be obtained using ac electric fields. This robust layered structure may offer a novel molecular matrix for separation and transport media, as well as a substrate for various molecular devices.

Acknowledgment. The authors would like to thank Dr. H. Körner for cooperation with real time X-ray experiments and valuable discussion of the results, Dr. J. Navaie and the Cornell High Energy Synchrotron Source (CHESS) staff for their marvelous technical support during the CHESS experiments, and the Cor-

nell Materials Science Center for use of their computer facilities. This research was partially supported by Japan Synthetic Rubber Co., Ltd. and the National Science Foundation.

References and Notes

(1) Barclay, G. G.; Ober, C. K. *Prog. Polym. Sci.* **1993**, *18*, 899.
(2) Broer, D. J.; Lub, J.; Mol, G. N. *Nature* **1995**, *378*, 467.
(3) Broer, D. J.; Gossink, R. G.; Hikmet, R. A. M. *Angew. Makromol. Chem.* **1990**, *183*, 45.
(4) Barclay, G. G.; McNamee, S. G.; Ober, C. K.; Papathomas, K. I.; Wang, D. W. *J. Polym. Sci., Part A: Polym. Chem. Ed.* **1992**, *30*, 1845.
(5) Jahromi, S. *Macromolecules* **1994**, *27*, 2804.
(6) Körner, H.; Shiota, A.; Bunning, T. J.; Ober, C. K. *Science* **1996**, *272* (5259), 252.
(7) Dubois-Violette, E.; de Gennes, P. G.; Parodi, O. *J. Phys.* **1971**, *32*, 305.
(8) Helfrich, W. *J. Chem. Phys.* **1969**, *51*, 4092.
(9) Meyer, R. B. *Phys. Rev. Lett.* **1969**, *22*, 918.
(10) Shiota, A.; Ober, C. K. *J. Polym. Sci., Part A: Polym. Chem.* **1996**, *34*, 1291.
(11) Alexander, L. E. *X-Ray Diffraction Methods in Polymer Science*, reprint ed.; Robert E. Krieger Publishing Co.: Huntington, New York, 1979.
(12) McNamee, S. G.; Bunning, T. J.; McHugh, C. M.; Ober, C. K.; Adams, W. W. *Liq. Cryst.* **1994**, *17*, 179.
(13) Hadad, D. K. In *Epoxy Resins*, 2nd ed.; May, C. A., Ed.; Marcel Dekker, Inc.: New York, 1988; pp 1089.
(14) Orsay Liquid Crystal Group. *Phys. Rev. Lett.* **1969**, *22*, 1361.
(15) Miesowicz, M. *Nature* **1946**, *158*, 27.
(16) Shiota, A.; Körner, H.; Ober, C. K. *Liq. Cryst.*, to be submitted for publication.
(17) Lin, Y. G.; Zhou, R.; Chien, J. C. W.; Winter, H. H. *Polymer* **1989**, *30*, 2204.
(18) Shiota, A.; Ober, C. K. *Polymer*, in press.
(19) de Jeu, W. H.; Goossens, W. J. A.; Bordewijk, P. *J. Chem. Phys.* **1974**, *61*, 1985.
(20) Jahromi, S.; Kuipers, W. A. G.; Norder, B.; Mijs, W. J. *Macromolecules* **1995**, *28*, 2201.
(21) Flory, P. J. *Principles of Polymer Chemistry*; Cornell University Press: Ithaca, NY, 1953; p 432.
(22) Hikmet, R. A. M.; Broer, D. J. *Polymer* **1991**, *32*, 1627.

MA961745L